Supplement for:

Region-specific Network Plasticity in Simulated and Living Cortical Networks: Comparison of the Center of Activity Trajectory (CAT) With Other Statistics

Zenas C. Chao, Douglas J. Bakkum and Steve M. Potter

S1: Simulated networks.

Features:

The Neural Circuit SIMulator (Natschlager et al., 2002) was used to produce five artificial neural networks as described previously (Chao et al., 2005). Briefly, 1,000 leaky-integrate-and-fire (LIF) model neurons with a total of 50,000 synapses were placed randomly in a 3mm by 3mm area (see figure 1(c)). All synapses were frequency-dependent (Markram et al., 1998; Izhikevich et al., 2004) to model synaptic depression. 70% of the neurons were excitatory, with spike-timing dependent plasticity (STDP) (Song et al., 2000). The other neurons were inhibitory (30%) (Marom and Shahaf, 2002). Neurons made many short synaptic connections but a few long ones as well (Segev and Ben-Jacob, 2000). The number of synaptic connections per neuron followed a Gaussian distribution and each neuron had 50 ± 33 synapses onto other neurons (no multiple synapses from one neuron to another). The conduction delay was proportional to the distance between somata, and the conduction velocity was set to be 0.3 m/s (Kawaguchi and Fukunishi, 1998). Gaussian random noise was introduced into each neuron independently as fluctuations in membrane voltage: 30% of the neurons ("self-firing neurons") had variance at a high enough level to initiate spikes (Latham et al., 2000), while the

rest exhibited only subthreshold fluctuations. An 8 by 8 grid of electrodes was included, 60 of these (except corner electrodes 11, 18, 81 and 88) were used for recording and stimulation as in a real MEA (figure 1(d)). A stimulation electrode stimulated 76 ± 12 (n= 5 simulated networks) of the closest model neurons.

Setup of network initial states:

All excitatory synaptic weights were initially set to 0.25 and could vary between zero and 0.5 due to STDP. At the maximal weight, each spike would have a 90% probability of evoking a spike in the post-synaptic neuron, due to its summation with intrinsic noise. The synaptic weights for the inhibitory connections were fixed at -0.25. The networks were run for 5 hours in simulated time until the synaptic weights reached a steady state. Most of the excitatory synaptic weights (92 ± 3%) in the 5 reference networks were less than 0.05 or greater than 0.45. This bimodal steady-state distribution of weights arose from the STDP rule, as previously observed by Song et al.(Song et al., 2000), and Izhikevich and Desai (Izhikevich and Desai, 2003). The set of synaptic weights after 5 hours of spontaneous activity stabilized, without external stimuli, and was used as the initial state for the corresponding reference network.

S2: Calculations of the statistics for experiments in simulations and living cultures.

The evoked responses within 100 msec (to include all evoked responses) after the stimuli of random probing sequences (RPSs) were used for calculations of the statistics. The dimensionalities of different statistics are shown in Table S1. For those statistics include temporal information (FRH, MI, SCCC, JPSTH, and CAT), responses within 100 msec were binned by a 5 msec moving time bin with 500 μsec time step. 500 μsec time step was used to obtain fine temporal resolution, since it was less than the occurrence of an action potential. 5 msec bin size was used to acquire action potentials on multiple electrodes within a single bin. Also, the same binning parameters were used for all statistics in simulations and in living cultures for fair comparison of their performance.

1. Simulations:

Firing Rate (FR)

This most commonly used statistic quantifies the intensity of the evoked responses. During each simulation, stimuli at each electrode occurred multiple times (10.0 ± 3.1 trials) in one RPS. FR for evoked responses to each stimulation electrode was calculated by averaging the number of spikes counted at each recording electrode over trials, producing a 60-dimensional vector.

Firing Rate Histogram (FRH)

FRH expands on FR by including temporal information. FRH from recording electrode E_k to the probing stimulus at electrode P_i, $FRH_{E_k}^{P_i}$, was the average number of spikes counted in a 5 msec moving time window with 500 μsec time

step over trials, which resulted in a 1X191 vector. FRH for evoked responses to stimulation electrode P_i was defined by joining $FRH_{E_k}^{P_i}$ from 60 recording electrodes together, which formed an 11,460-dimensional (191X60) vector.

Center of Activity Trajectory (CAT)

The definition of CAT is described in Methods (Equation 1 and 2). The X and Y components are both 1X191 vectors. By appending two components together, CAT for evoked responses to each stimulation electrode was a 382-dimensional (191X2) vector.

Mutual Information (MI)

MI quantifies the statistical dependence, including higher order moments in addition to 2nd order, between responses at different locations (Moddemeijer, 1989; Brunel and Nadal, 1998; Paninski, 2003). MI between two recording electrodes E_k and E_j for stimulation electrode P_i is defined as the mutual information between two distributions: $FRH_{E_k}^{P_i}$ and $FRH_{E_j}^{P_i}$. Let $FRH_{E_k}^{P_i} = \{A_n\}_{n=1}^{191}$ and $FRH_{E_j}^{P_i} = \{B_m\}_{m=1}^{191}$, where A_n and B_m represent elements in *FRH*s. Then the MI between $FRH_{E_k}^{P_i}$ and $FRH_{E_j}^{P_i}$ is defined as:

$$I(FRH_{E_k}^{P_i}, FRH_{E_j}^{P_i}) = \sum_{n,m} P_{X,Y}(A_n \times B_m) \ln \frac{P_{X,Y}(A_n \times B_m)}{P_X(A_n) \times P_Y(B_m)}$$

where P_X and P_Y represent the marginal probabilities of $FRH_{E_k}^{P_i}$ and $FRH_{E_j}^{P_i}$, and $P_{X,Y}$ represents the joint probability of $FRH_{E_k}^{P_i}$ and $FRH_{E_j}^{P_i}$. MI was estimated by using the histogram-based mutual information methods described by Moddemeijer (Moddemeijer, 1989). In this study, the MATLAB codes from

Rudy Moddemeijer's group were used[1]. MI provides a non-directional connectivity map, which represents the dependence between activities at different pairs of electrodes. By joining the MI from every pair of electrodes, MI for evoked responses to each stimulation electrode was a 1,770-dimensional (60X59/2) vector.

Shift-predictor Corrected Cross-Correlogram (SCCC)

The corrected cross-correlogram (Michalski et al., 1983; Eggermont, 1992; Brody, 1999; Franco et al., 2004; Ventura et al., 2005) removes the peak in the original cross-correlogram that is due to co-stimulation of the neurons, and measures the association between neurons. For each pair of recording electrodes, the "raw" cross-correlogram was constructed by averaging the cross-correlograms between two spike trains from the two electrodes over trials. The "shift predictor" was constructed by averaging the cross-correlograms between all possible pairs of spike trains from the two electrodes but from different trials. SCCC was then the raw cross-correlogram minus the shift predictor. In this study, the algorithm described by George Gerstein's group was used[2].

With the same binning resolution used for FRH, SCCC between each pair of recording electrodes was a (191X2-1)-dimensional vector which represents the correlations sequence at different lags. Therefore, SCCC for evoked responses to each stimulation electrode was a 674,370-dimensional ((191X2-1)X60X59/2) vector.

[1] http://www.cs.rug.nl/~rudy/papers/abstracts/RM8902.html
[2] http://mulab.physiol.upenn.edu/crosscorrelation.html

Joint Peri-Stimulus Time Histogram (JPSTH)

The JPSTH quantifies the causality between responses at different locations (Gerstein and Perkel, 1969; Aertsen et al., 1989; Ventura et al., 2005). JPSTH finds the fixed delay between sequences of spikes recorded at different pairs of neurons (electrodes) over multiple trials, which can depict causal relationships between them. Similar to SCCC, the shift-predictor was applied on the "raw" JPSTH to eliminate the time-locked stimulus-induced covariation due to co-stimulation. In this study, the algorithm and MATLAB codes from George Gerstein's group were used[3]. The results can provide directional information about the connectivity. With the same binning resolution used for FRH, JPSTH between each pair of recording electrodes was 191X191-dimensional. Therefore, JPSTH for evoked responses to each stimulation electrode was a 64,571,370-dimensional (191X191X60X59/2) vector.

Center of Activity Trajectory with Electrode Locations Shuffled (CAT-ELS)

The electrode locations, E_k, were randomly shuffled. Then CAT-ELS was calculated according to Equation 1 and 2 (in Methods) by using these shuffled electrode locations. For each network, the electrode locations were shuffled 10 times and 10 different corresponding CAT-ELSs were generated.

2. Experiments in living cultures:

Firing Rate (FR)

The number of spikes was counted at each recording electrode for each probe response and averaged every block. Thus, for each stimulation electrode, a

[3] http://mulab.physiol.upenn.edu/jpst.html

60-dimensional FR vector was obtained for every 240 sec ("block", see Methods).

Firing Rate Histogram (FRH)

For evoked responses to each stimulus, the FRH was calculated by using a 5 msec moving time window with time step of 500 μsec. Thus, for each stimulation electrode, an 11,460-dimensional (191X60) FRH vector was obtained for every block.

Center of Activity Trajectory (CAT)

Let $FRH_{E_k}^{P_i}$ be the average responses over each block, recorded at electrode E_i to stimulation electrode P_i. CAT for stimulation electrode P_i was then calculated from the $FRH_{E_k}^{P_i}$ by using Equation 1 and 2 (in Methods). Thus, for each stimulation electrode, a 382-dimensional (191X2) CAT vector was obtained for every block.

Shift-predictor Corrected Cross-Correlogram (SCCC)

With the same binning resolution used for FRH, SCCC between each pair of recording electrodes was calculated for every block. Thus, for each stimulation electrode, a 674,370-dimensional ((191X2-1)X60X59/2) SCCC vector was obtained for every block.

Center of Activity Trajectory with Electrode Locations Shuffled (CAT-ELS)

CAT-ELS was calculated by the same shuffling procedure used in simulations. For each experiment, the electrode locations were shuffled 10 times and 10

different corresponding CAT-ELSs were generated. The dimensionality of CAT-ELS was the same as CAT.

Table S1. The dimensionality of the statistics.

Statistics	Dimensionality[1]	
	Simulations	Experiments in living cultures
FR	60	60
FRH	11,460	11,460
MI	1,770	-
CAT	382	382
CAT_ELS	382	382
SCCC	674,370	674,370
JPSTH	64,571,370	-

[1] The dimensionality is defined as the length of the statistic calculated from evoked responses to *one* stimulation electrode in one simulation or in one block (for experiments in living cultures).

S3: Movie of CATs in a simulated network.

Different patterns of CATs were obtained from evoked responses to stimuli at different electrodes in simulation (see **Movie S3**). **A.** The rasterplot of 1 second of network activity from 1000 LIF neurons. Evoked responses to stimuli at different electrodes are shown in different colors. **B.** 1000 neurons on 3mm by 3mm area. Neurons are shown as gray dots, and the active synapses are shown in cyan lines. The locations of stimulation electrodes are indicated by crosses with the corresponding colors shown in A. **C.** The corresponding CATs. The color of the trajectory represents the corresponding evoked response shown in A. Time is represented in the red bar at the bottom of A.

S4: Performances of the 6 statistics after spike sorting in simulated networks.

Sorting recorded action potentials and recalculating the activity statistics improved the performance of all except for CAT. However, the CAT still showed the highest performance. The calculation of the CAT remained the same as the sorted spikes are spatially summed according to recording electrode locations The six statistics were re-calculated based on the activity of about 250 spike sorted neurons instead of 60 electrodes (see Results).JPSTH, SCCC, FRH, MI and FR improved 11.1, 17.6, 11.0, 35.0 and 31.2 %, respectively. The same figure representation was used as in Figure 7. The sensitivities and specificities for these statistics (also see Discussion) are shown in the table.

Statistic	*CAT*	*JPSTH*	*SCCC*	*FRH*	*MI*	*FR*
Sensitivity (%)	88.7	85.4	82.8	60.2	65.0	51.2
Specificity (%)	82.4	77.9	77.9	85.3	95.6	100

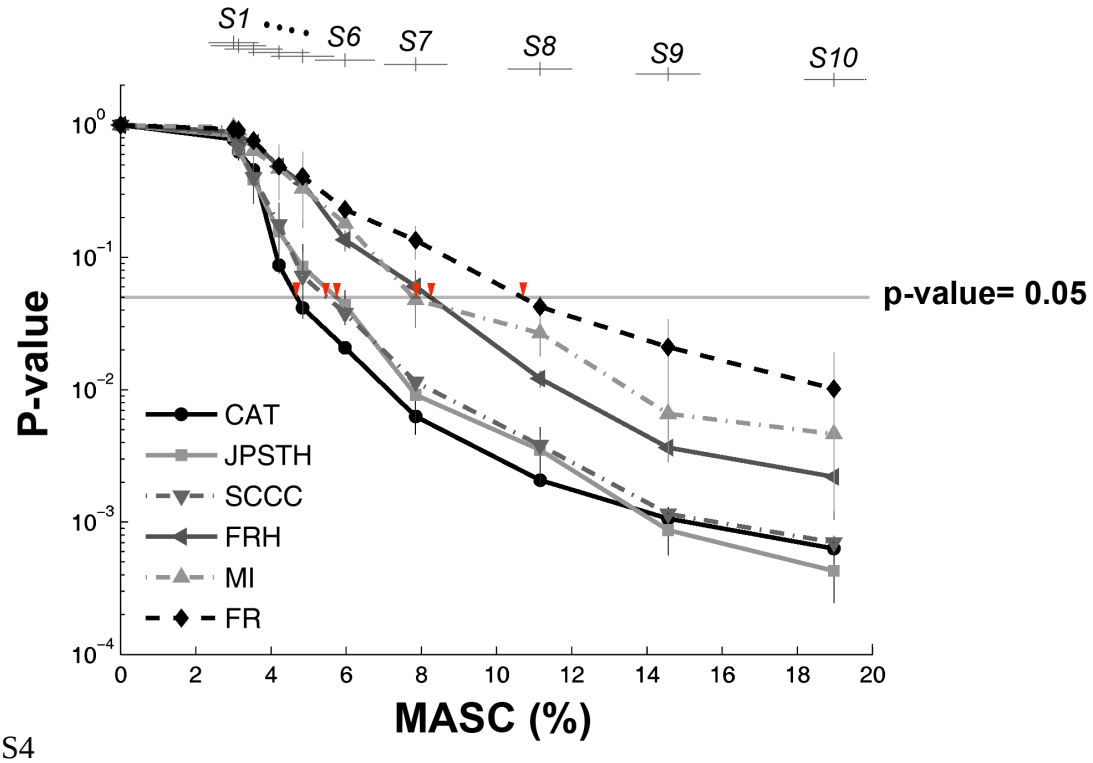

Figure S4

S5: Movies of CATs in a MEA culture: before and after tetanization.

Different patterns of CATs were obtained from evoked responses to different probe electrodes in MEA cultures. Also, CATs from the same probe electrode were found different before and after tetanization (shown **Movie S5a** and **Movie S5b**, respectively). **A.** The rasterplot of 10 seconds of network activity at 60 electrodes. Evoked responses to different probe electrodes are shown in different colors (the same color was used for the same probe electrode in 2 movies). **B.** Activity distribution in 60-channel MEA. Activity intensity at different electrodes is shown by black filled circles with different sizes. The locations of probe electrodes are indicated by crosses with the corresponding colors shown in A. **C.** The corresponding CATs. The color of the trajectory represents the corresponding evoked response shown in A. The scales in the 2 movies are the same. Time is represented in the red bar at the bottom of A.

S6: CATs in all experiments in MEA cultures: before and after tetanization.

Different patterns of CATs were obtained before and after tetanization from 6 experiments in MEAs (see figure). CATs obtained before tetanization (*Pre*) and after tetanization (*Post*) for each probe electrode are shown. The column-row numbers of corresponding probe electrodes are shown in the 8 by 8 MEA grids shown in the middle. The tetanization electrodes are depicted by thick black circles. For each probe, CATs calculated for each "block" (see Methods) are shown in black lines and overlaid. The averaged CATs are shown in colored circles (from blue to red).

092705_A

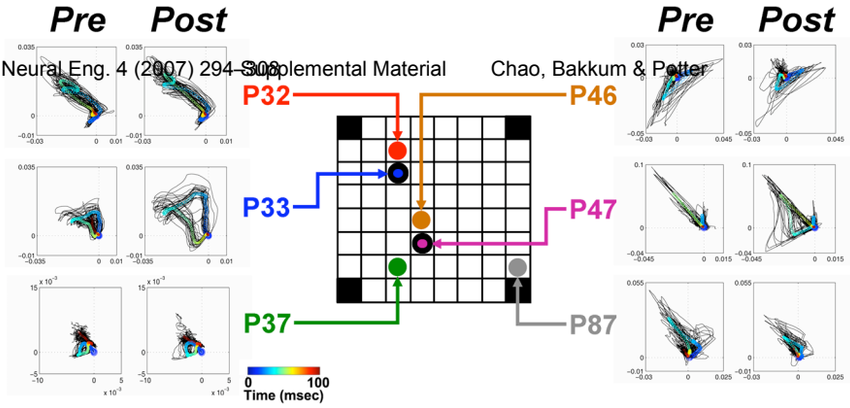

092605_B

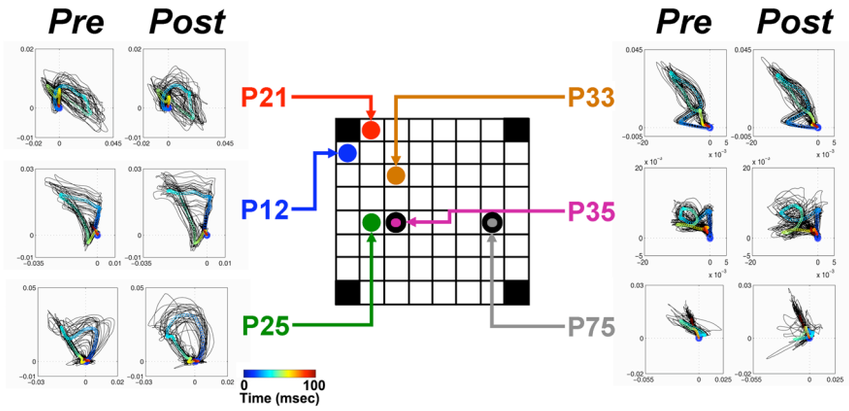

030106_F

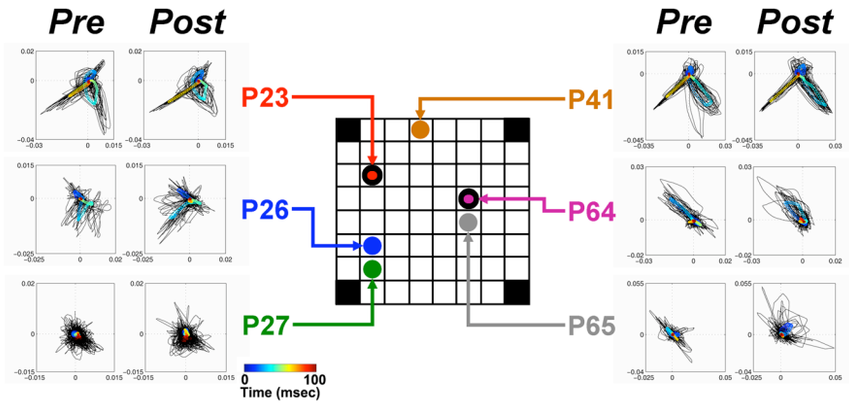

030206_B

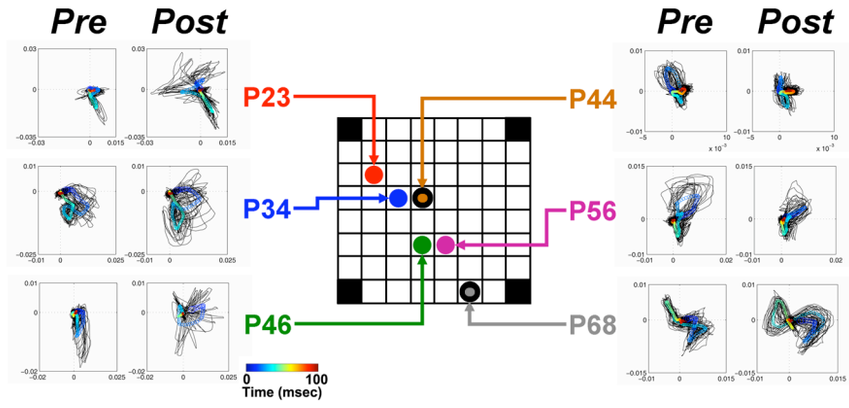

091905_A

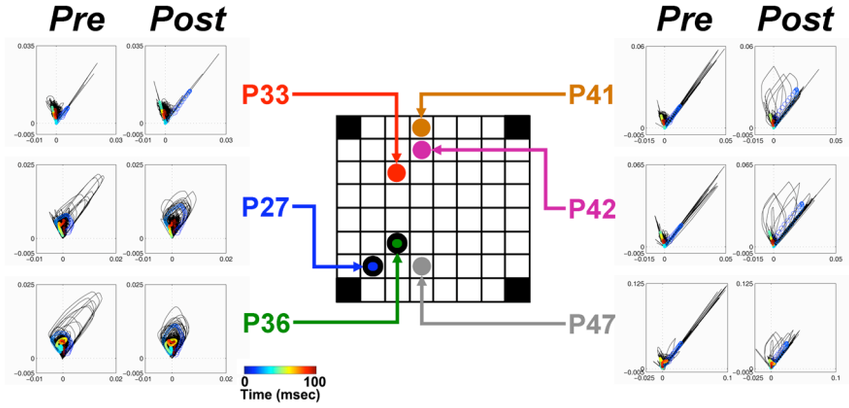

090705_A

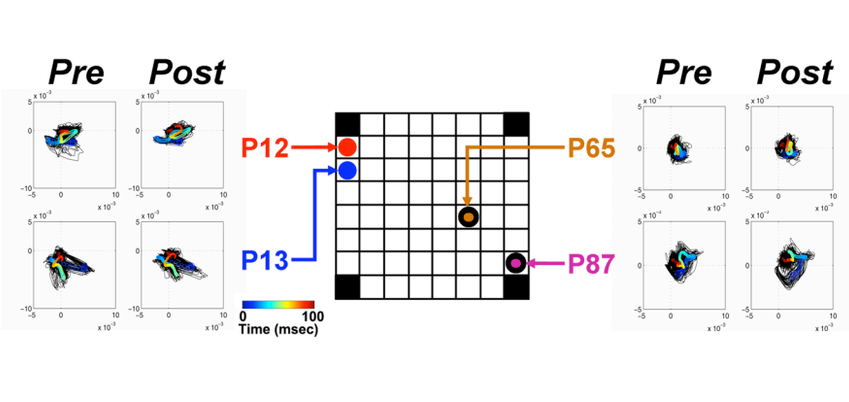

S7: Calculation of center of weights (CW) for simulations.

Plastic changes in the simulated networks' functional architecture can be represented by the trajectory of the center of weights (CW). Let $W_i(t)$ be the weight of synapse i at time t. Let X_i and Y_i indicate the horizontal and vertical distances from the post-synaptic neuron of the synapse i to a reference point (the center of the dish was used). Then, CW of time t is a two dimensional vector:

$$\vec{CW}(t) = \frac{\sum_{i=1}^{N} W_i(t) \cdot [X_i, Y_i]}{\sum_{i=1}^{N} W_i(t)}$$

where N is the total number of excitatory synapses. Note that while CAT describes the spatiotemporal patterns of signal propagation, CW shows the dynamics of connection strengths.

References

Aertsen AM, Gerstein GL, Habib MK, Palm G (1989) Dynamics of neuronal firing correlation: modulation of "effective connectivity". J Neurophysiol 61:900-917.

Brody CD (1999) Correlations Without Synchrony. Neural Computation 11:1537-1551.

Brunel N, Nadal J-P (1998) Mutual Information, Fisher Information, and Population Coding. Neural Computation 10:1731-1757.

Chao ZC, Bakkum DJ, Wagenaar DA, Potter SM (2005) Effects of random external background stimulation on network synaptic stability after tetanization—A modeling study. Neuroinformatics 3:263-280.

Eggermont J (1992) Neural interaction in cat primary auditory cortex. Dependence on recording depth, electrode separation, and age. J Neurophysiol 68:1216-1228.

Franco L, Rolls ET, Aggelopoulos NC, Treves A (2004) The use of decoding to analyze the contribution to the information of the correlations between the firing of simultaneously recorded neurons. Exp Brain Res 155:370-384.

Gerstein G, Perkel D (1969) Simultaneously recorded trains of action potentials: analysis and functional interpretation. Science 164:828-830.

Izhikevich EM, Desai NS (2003) Relating STDP to BCM. Neural Computation 15:1511-1523.

Izhikevich EM, Gally JA, Edelman GM (2004) Spike-Timing Dynamics of Neuronal Groups

Cerebral Cortex 14:933-944.

Kawaguchi H, Fukunishi K (1998) Dendrite classification in rat hippocampal neurons according to signal propagation properties - Observation by multichannel optical recording in cultured neuronal networks. Experimental Brain Research 122:378-392.

Latham PE, Richmond BJ, Nirenberg S, Nelson PG (2000) Intrinsic dynamics in neuronal networks. II. Experiment. Journal of Neurophysiology 83:828-835.

Markram H, Gupta A, Uziel A, Wang Y, Tsodyks M (1998) Information processing with frequency-dependent synaptic connections. Neurobiology of Learning and Memory 70:101-112.

Marom S, Shahaf G (2002) Development, learning and memory in large random networks of cortical neurons: Lessons beyond anatomy. Quarterly Reviews of Biophysics 35:63-87.

Michalski A, Gerstein GL, Czarkowska J, Tarnecki R (1983) Interactions between cat striate cortex neurons. Experimental Brain Research 51:97 - 107.

Moddemeijer R (1989) On Estimation of Entropy and Mutual Information of Continuous Distributions. Signal Processing 16:233-246.

Natschlager T, Markram H, Maass W (2002) Computer models and analysis tools for neural microcircuits. In: A Practical Guide to Neuroscience Databases and Associated Tools.

Paninski L (2003) Estimation of Entropy and Mutual Information. Neural Computation 15:1191-1253.

Segev R, Ben-Jacob E (2000) Generic modeling of chemotactic based self-wiring of neural networks. Neural Networks 13:185-199.

Song S, Miller KD, Abbott LF (2000) Competitive hebbian learning through spike-timing-dependent synaptic plasticity. Nature Neuroscience 3:919-926.

Ventura Vr, Cai C, Kass RE (2005) Trial-to-Trial Variability and Its Effect on Time-Varying Dependency Between Two Neurons. J Neurophysiol 94:2928-2939.